RESEARCH ARTICLE

Finite element modeling of grasping porous materials in robotics cells

Roman Mykhailyshyn[1,2,3,4] (ID), Ann Majewicz Fey[5,6] and Jing Xiao[2]

[1]Texas Robotics, College of Natural Sciences and the Cockrell School of Engineering, The University of Texas at Austin, Austin, TX, USA, [2]Department of Robotics Engineering, Worcester Polytechnic Institute, Worcester, MA, USA, [3]EPAM School of Digital Technologies, American University Kyiv, Kyiv, Ukraine, [4]Department of Automation of Technological Processes and Manufacturing, Ternopil Ivan Puluj National Technical University, Ternopil, Ukraine, [5]Walker Department of Mechanical Engineering, The University of Texas at Austin, Austin, TX, USA, and [6]Department of Surgery, UT Southwestern Medical Center, Dallas, TX, USA
Corresponding author: Roman Mykhailyshyn; Email: roman.mykhailyshyn@austin.utexas.edu

Abstract

Handling and manipulating flexible porous objects is one of the main challenges in robotics for household and industrial tasks. Improving the design of grippers for flexible objects of manipulation is an important stage in the development of this topic. This article proposes a method of modeling a gripper for porous objects using the finite element method. It identifies the main parameters of the model that will affect the grasping force and the permeability of porous objects. The power characteristics of the obtained gripper model for different supply pressures, with varying porosity of the manipulated objects, are determined. The obtained characteristics are then used to find the correspondence of channel length for three textile materials with different permeable properties. An experimental study of the lifting force is conducted, and a comparison is made with the obtained modeling data for the presented samples. Additionally, using the obtained simulation data, an analysis of the pressure distribution on the surface of the porous object of manipulation is performed. As a result, it is found that the gripping device must use a design with elements to stabilize the distribution of pressure in its chamber, which will increase the stability of the gripping process.

1. Introduction

Grasping and manipulating flexible objects is an important task within the scientific community, as such tasks present numerous challenges. The most popular tasks in this field, tackled by researchers, include modeling deformation of objects [1], developing adaptive gripping systems [2], substantiating manipulation methods [3–6], developing gripping devices for specific types of flexible materials [7–11], studying the dynamics of manipulating flexible objects [12], incorporating machine vision for manipulation of flexible objects [13, 14], investigating material deformations using torque sensors [15], and many others. These challenges are increasingly prevalent with the growing presence of robotics in human environments. Consequently, the utilization of collaborative robots equipped with artificial vision systems and the ability to interact with flexible objects is becoming more common [16, 17]. Moreover, the automation of modern production and warehousing operations has long necessitated the handling of flexible objects [18, 19].

By analyzing reviews of grippers and applications for manipulating flexible objects [19–25] in robotic systems, it becomes apparent that many problems can be more easily solved by using specialized grippers designed for specific types of flexible materials. One of the most challenging materials to grip and manipulate is textiles and their products. This difficulty arises from the distinct properties exhibited by textile materials, such as deformation and permeability, which vary depending on factors such as
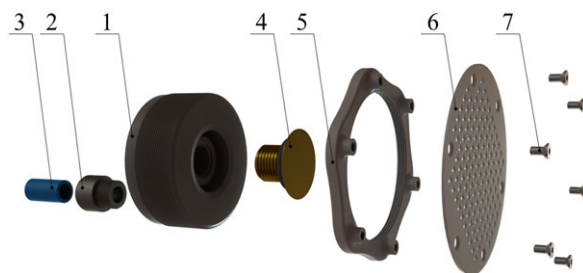
Figure 1. *Gripper design for flexible and porous objects [28] (1 – housing, 2 – fitting, 3 – compressed pressure supply hose, 4 – conical insert, 5 – holder, 6 – anti-vibration insert, and 7 – anti-vibration mounting bolts).*

manufacturing method, shape, and processing [15, 26]. Consequently, the development of grippers and the modeling of gripping and manipulation processes for textile materials have emerged as promising areas of research.

It has become a widespread practice to model and investigate the process of gripping flexible objects using mechanical gripping devices [1, 8, 27]. However, an article [28] states that certain jet grippers, such as the one described in the article, make it much easier to handle flexible objects, particularly textiles. This ease is attributed to the ability of these grippers to grip objects from a distance and in various orientations. This advantage is achieved through the design of the Bernoulli ejection gripping device. Bernoulli gripping devices (BGDs), in general, possess unique properties that set them apart from other grippers [29–31]. One notable application of BGDs is in food grasping and manipulation [32–34]. The first person to study the deformation caused by BGD on flexible objects was Prof. Brun and Melkote [35, 36], and further development in this area can be found in the paper [37]. Furthermore, modifications of the BGD have been developed to grip leather products [38] and for organ gripping during laparoscopy [39].

Numerous papers [40–50] have been dedicated to the modeling of Bernoulli gripper. The article [43] provides a substantiation of the shape and parameters of the gripper's friction elements to ensure maximum lifting force. Additionally, it demonstrates the impact of gripping parameters on the positioning precision of objects during handling operations [44]. It is worth noting that BGDs exhibit high dynamic characteristics, enabling contactless manipulation of objects [45, 46]. The process of manufacturing and prototyping Bernoulli traps also has an important effect on their technical characteristics, which is explored in paper [51]. Most of the scientific papers [47–50] are dedicated to the optimization and substantiation of BGD design parameters using various modeling methods. However, the modeling of grippers for flexible materials with pores, such as textiles, has not been addressed. The authors of the article [28] proposed a gripping device for flexible and porous objects, based on the BGD (Fig. 1).

One notable feature of this gripper is the inclusion of an anti-vibration insert (labeled as 6), which effectively reduces the vibration of the manipulated flexible object. This gripper device enables the grasping of objects from a significantly greater distance compared to the traditional ejection gripper. Moreover, the orientation of the manipulated object in space is not critical during the grasping process, thus making this technology suitable for uncertain conditions.

However, this gripper designed for flexible and porous objects is not optimal in terms of technical characteristics. Therefore, in this article, the authors first propose a model that utilizes the finite element method (FEM) to simulate the operation of the gripping device for flexible and porous materials. The developed method's adequacy is verified by comparing the obtained data with experimental studies. Using this model, the authors identify the parameters that influence the gripping process. Based on the
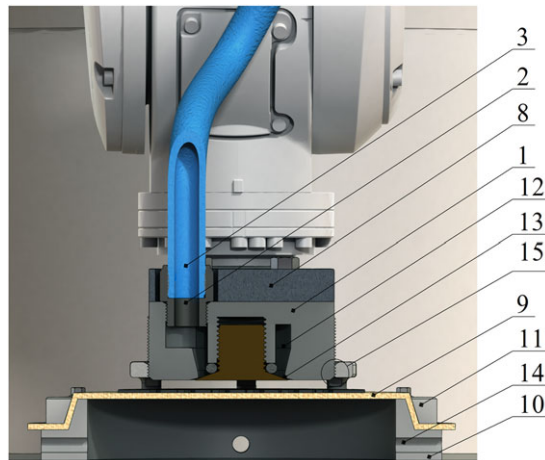
Figure 2. *Experimental configuration for determining the grasping force for flexible and porous objects of manipulation [28] (1 – gripper body, 2 – fitting, 3 – housing, 8 – connector, 9 – textile material, 10 – bottom board attached to scales, 11 – the top plate fastening textiles to the bottom plate, 12 – the chamber of the gripping device, 13 – an annular nozzle of the gripper, 14 – devacuumation openings, and 15 – threaded connection of the holder and the case of the gripper).*

analysis of the gripper's design impact on its power characteristics, the authors suggest modifications to the compressed air supply system for the gripper chamber. Modifying the gripper design enables the prevention of object displacement during grasping.

2. Materials and methods

To check the adequacy and calibration of the developed model, experimental studies of the device for grasping flexible and porous objects were conducted using the method proposed by the authors in the article [28]. This method involves determining the grasping force for each type of material that will be used as the manipulated object (Fig. 2).

The experimental configuration consists of an industrial robot with a gripping device for flexible and porous objects fixed on the flange using connector label 8. The gripping device approaches the textile material (labeled as 9). The material is secured to the bottom plate (labeled as 10), which is then connected to a weight (with an accuracy of ± 1 g). When pressure is applied through the hose (labeled as 3) to the gripper chamber (labeled as 12), air flows through the annular nozzle (labeled as 13). The ejection effect under the conical insert creates a vacuum, resulting in air being suctioned through the pores of the insert. This leads to the creation of a pressure difference in the area of application of the gripper and beyond it. To measure the grasping force, the gripper moves vertically upwards relative to the manipulated object, and the maximum lifting force value is recorded during the movement.

Thanks to the design of the gripping device, it is possible to adjust the gap between the insert (labeled as 6) and the gripping device from 0.3 mm to 4 mm. The pressure in the gripping chamber is adjusted from 15 to 200 kPa using a pressure reducer. During the study, the following parameters of the gripper were kept constant: the radius of the insert (4) is 15 mm, the radius of the gripper is 30 mm, the angle of the insert (4) is 20°, and the height of the conical insert at the thinnest point is 0.1 mm.

A digital 3D scanning profilometer was utilized to analyze the parameters of the material. Two plain weave fabrics were chosen, each exhibiting distinct characteristics [52]: Polyester 6 (Fig. 3(a)) – thread width from 0.2 mm to 0.23 mm, pore width and height from 0.01 mm to 0.055 mm; Flannel 3 (Fig. 3(b)) – thread width from 0.2 mm to 0.4 mm, and visible pores are almost absent. The parameters of the surface
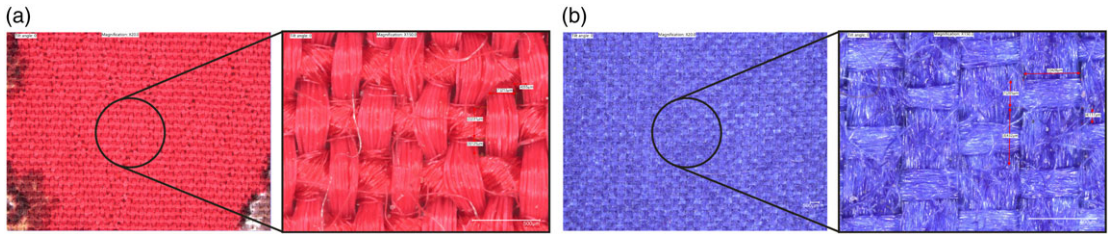
Figure 3. *Studied material [52] plain weave (x20 and x150): (a) Polyester 6; (b) Flannel 3.*
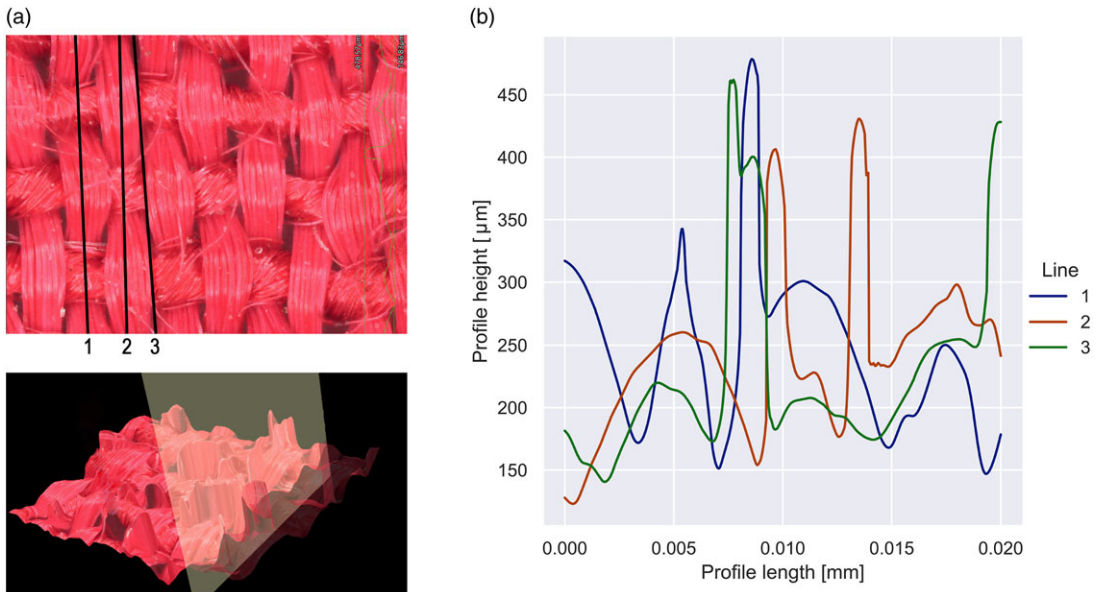

Figure 4. *Textile surface profile Polyester 6: (a) 3D drawing of a textile surface profile; (b) Graph of the obtained profile along three lines.*

profile of the textile materials were determined using a 3D scanning microscope, Keyence VHX-70000 (Fig. 4).

From Fig. 4, the profile of the material is uneven due to weaving and has a depth of μm in this case. It is challenging to accurately replicate the geometry of the textile material, including all the three-dimensional pores. Therefore, to account for the porosity of the threads and significant deviations in the profile of the textile material, a simplified model of porosity is proposed. In the simulation, a camera (with height H) is utilized to represent the porous material. The camera is positioned beneath the anti-vibration nozzle and has the same diameter as the gripping device (refer to Fig. 5).

A channel with a variable diameter D and length L is connected to the chamber, simulating a porous object. By adjusting these parameters, the permeability of the manipulation object (textile) can be controlled. The grasping force is measured at the average height of the chamber, which is $H/2$. This choice is based on the fact that the pressure in the middle section area is the most stable and represents the average value. An anti-vibration insert with 50% plastic filling for 3D printing was selected for the simulation. The specific parameters of the grid insert, such as line width of 0.5 mm and hole size of 1×1 mm, were determined using microscopy.

The mathematical model for the flow of air in the gap between the gripper and insert is defined on the RANS equations [53, 54]. The modeling utilized the Shear Stress Transport (SST) turbulence model [55] and the γ-model of laminar-turbulent transition [56, 57].
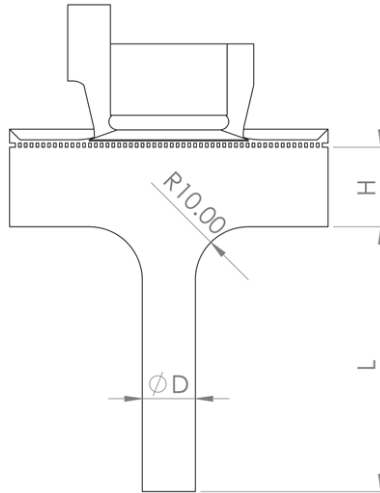
Figure 5. *The schematic diagram for modeling a gripping device for flexible and porous objects.*

The γ-model of laminar-turbulent transition is described by a single differential equation governing the interdependence coefficient γ:

$$\frac{\partial(\rho\gamma)}{\partial t} + \frac{\partial(\rho v_j \gamma)}{\partial x_j} = P_\gamma - E_\gamma + \frac{\partial}{\partial x_j}\left[\mu + \left(\frac{\mu_t}{\sigma_\gamma}\right)\frac{\partial\gamma}{\partial x_j}\right], \tag{1}$$

where ρ is the air density; t is the time; x is the coordinate; v is the vector of air velocity; P_γ, E_γ are, respectively, generative and dissipation members of managing directors of laminar and turbulent transition; μ is the molecular dynamic viscosity of gas; μ_t is the turbulent dynamic viscosity of gas; and $\sigma_\gamma = 1.0$ is the model constant.

The transition model uses modified equations of the SST model:

$$\frac{\partial}{\partial t}(\rho k) + \frac{\partial}{\partial x_j}(\rho v_j k) = \tilde{P}_k + P_k^{\lim} - \tilde{D}_k + \frac{\partial}{\partial x_j}\left((\mu + \sigma_k \mu_t)\frac{\partial k}{\partial x_j}\right), \tag{2}$$

$$\frac{\partial}{\partial t}(\rho\omega) + \frac{\partial}{\partial x_j}(\rho v_j \omega) = \alpha\frac{P_k}{v_t} - D_\omega + Cd_\omega + \frac{\partial}{\partial x_j}\left((\mu + \sigma_\omega \mu_t)\frac{\partial\omega}{\partial x_j}\right), \tag{3}$$

where k is the kinetic turbulent energy; ω is the specific speed of dissipation of kinetic energy of turbulence; P_k, D_k are the original generation and dissipation of the SST model; $P_k^{\lim}$ is the additional part, which provides the correct gain of turbulent viscosity in transitional area at very low level of turbulent viscosity of the running stream; v_t is the turbulent kinematic viscosity of gas; and σ_k, α, a_1 are the empirical constants of model.

3. Results and discussion

Based on the gripper design, a model of the grasping process of flexible and porous objects was developed, incorporating specific boundary conditions for the airflow (Fig. 6).

There are several types of solvers using SST turbulence models in Ansys-CFX. Therefore, was conducted the study of the influence elements e_s of the grid between adjacent planes on the grasping force (Fig. 7). Changing this parameter in turn changes the number of e mesh grid elements. For this modeling, the inlet pressure is $p_0 = 100\,\text{kPa}$, $H = 20\,\text{mm}$, $D = 3\,\text{mm}$, and $L = 50\,\text{mm}$, and the gap between the insert and the gripper is $h_1 = 0.6\,\text{mm}$.
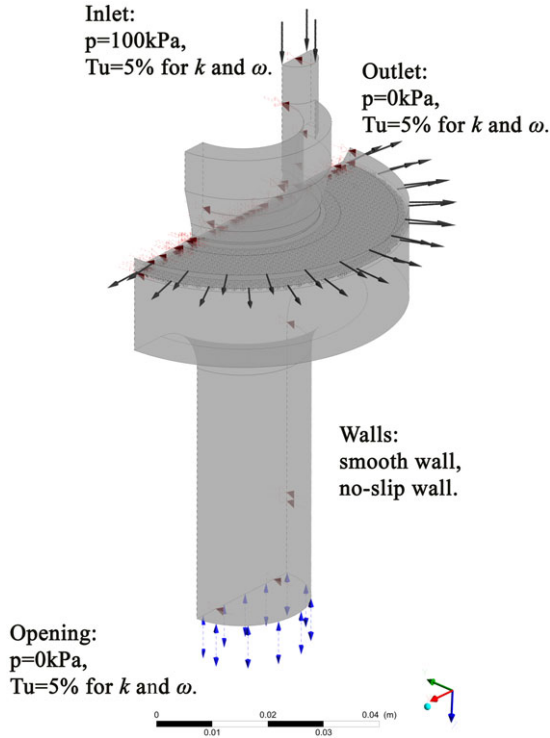
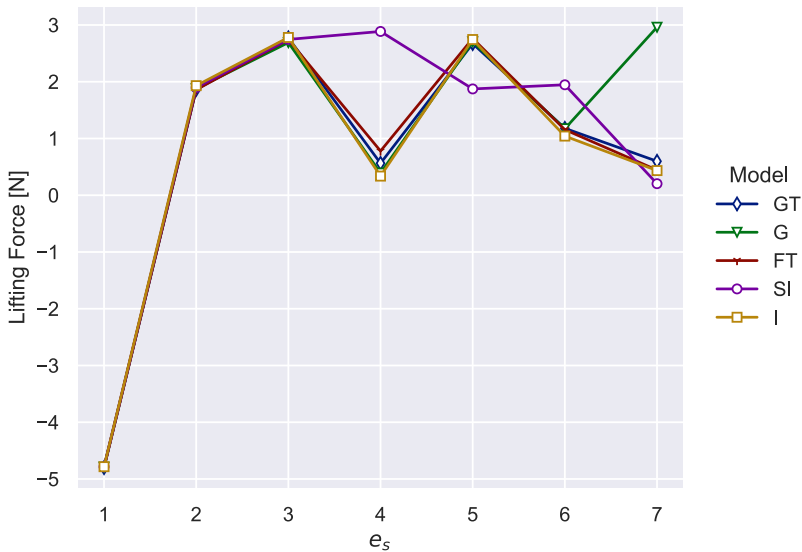**Figure 6.** *Boundary conditions for air flow model.*

Figure 7. *Influence of the number of grid elements on the lifting force of the gripper (GT – gamma theta, G – gamma, FT – fully turbulence, SI – special intermediately, and I – intermediately).*
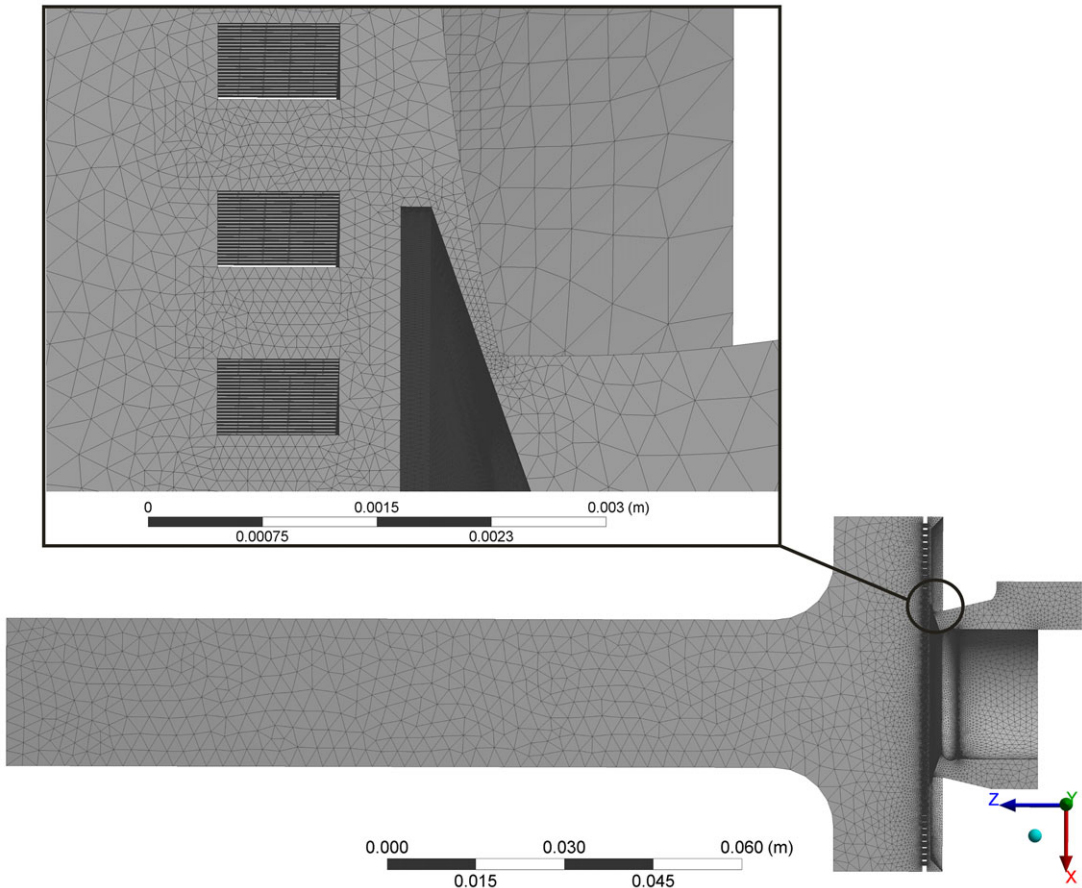
Figure 8. *Mesh grid of final elements of air flow.*

Several types of solvers that utilize SST turbulence models in Ansys-CFX are available. Therefore, a study was conducted to examine the influence of the number of grid elements e_s between adjacent planes on the grasping force (Fig. 7). By modifying this parameter, the number of mesh grid elements is altered accordingly. In this modeling study, the following parameters were used: inlet pressure $p_0 = 100$ kPa, $H = 20$ mm, $D = 3$ mm, and $L = 50$ mm, and the gap between the anti-vibration insert and the gripper is $h_1 = 0.6$ mm.

As depicted in Fig. 7, the lifting force remains constant for all models up to $e_s = 3$, while only the SI model achieves the maximum value at $e_s = 4$. The remaining models reach their maximum lifting force at $e_s = 5$; hence, the SI model at $e_s = 4$ will be utilized for future modeling. The number of mesh grid elements will vary based on changes in parameters H, D, and L (Fig. 8). It has been determined that the average number of volume elements in the mesh grid is 7.4 million, with a total of 1.4 million nodes in the working area.

For further investigation, the modeling includes examining the impact of changing the height of the chamber (H) on the grasping force and the airflow through the channel connected to the chamber (Fig. 9).

As observed in Fig. 9, the grasping force increases as the height of the chamber (H) is raised, with a corresponding increase in pressure within the 5–20 mm range. In other cases, the model exhibits inappropriate behavior. Conversely, an increase in pressure should result in a proportional increase in airflow rate. This behavior is characteristic of a chamber height exceeding 10 mm. These characteristics accurately describe the operational model of the gripping device within the 10–20 mm range. Consequently, a height of $H = 15$ mm, representing the midpoint of this range, was selected for further studies.
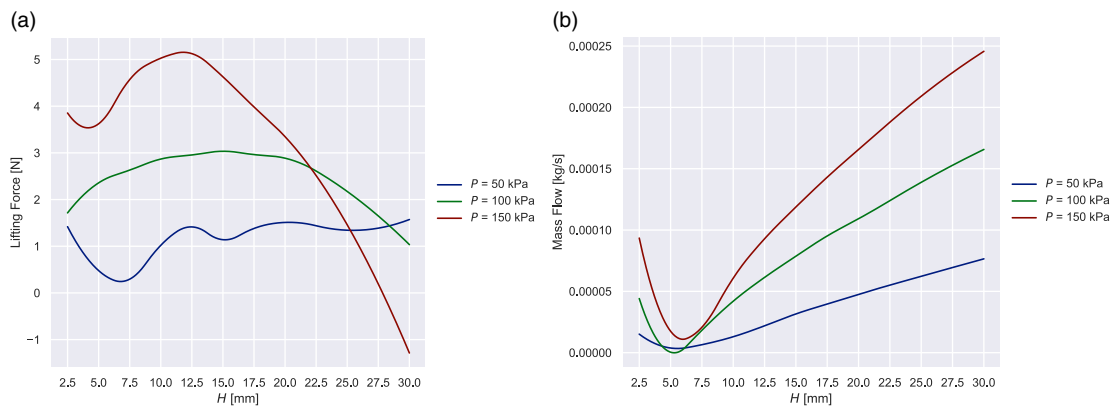
Figure 9. *The effect of the height of the model chamber on: (a) the lifting force of the gripper and (b) air flow through the channel.*
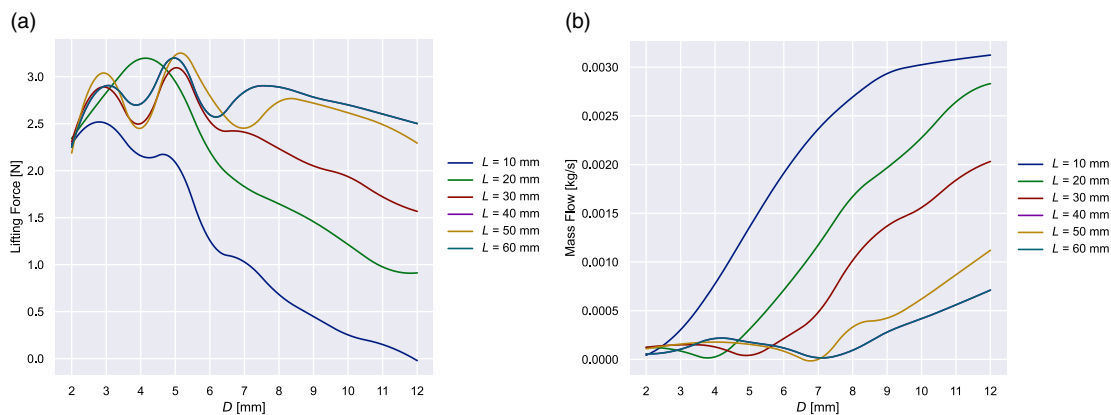

Figure 10. *The effect of the diameter of the model channel on: (a) the lifting force of the gripper and (b) air flow through the channel.*

By adjusting the parameters of the diameter (D) and length (L) of the channel connected to the chamber, it becomes possible to modify the airflow through the textile material while maintaining a constant supply pressure of $p_0 = 100\,\text{kPa}$ (Fig. 10).

From Fig. 10, the grasping force is not stable when the channel diameter is up to 8 mm. To ensure adequacy, it is necessary for the lifting force to increase with increasing channel length while keeping the diameter constant, resulting in reduced air consumption. This is because increasing the length of the channel increases the energy consumption of air due to friction forces on the passage of a longer section of the channel. This trend begins to manifest itself with a channel diameter of more than 8 mm. To verify the linearity of the characteristic, a study of the influence of the channel length L at $D = 12\,\text{mm}$ on the lifting force (Fig. 11(a)) was conducted with L ranging from 20 mm to 220 mm.

From Fig. 11(a), it is evident that the lifting force does not exhibit a linear characteristic and has an underestimated value in the range $L = 100 \ldots 160\,\text{mm}$. The same characteristic is observed with smaller channel diameters. Therefore, to study the linearity of the lifting force characteristic (Fig 11(b)), the influence of the channel length $L = 40 \ldots 240\,\text{mm}$ was further examined at different diameters ranging from $D = 10 - 40\,\text{mm}$ and a constant supply pressure of $p_0 = 100\,\text{kPa}$.

The greatest linearity of the grasping force is observed (Fig 11(b)) within the range of channel length $L = 40 - 200\text{mm}$, with a channel diameter of $D = 25\,\text{mm}$. Therefore, for further research, the proposed
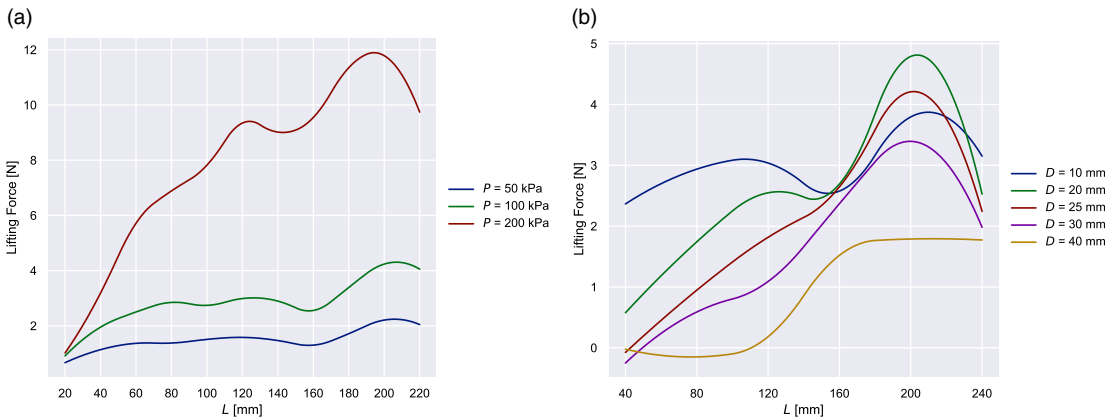
Figure 11. *Influence of channel length on the lifting force of the gripper: (a) at various supply pressures and (b) at various diameters of the channel.*
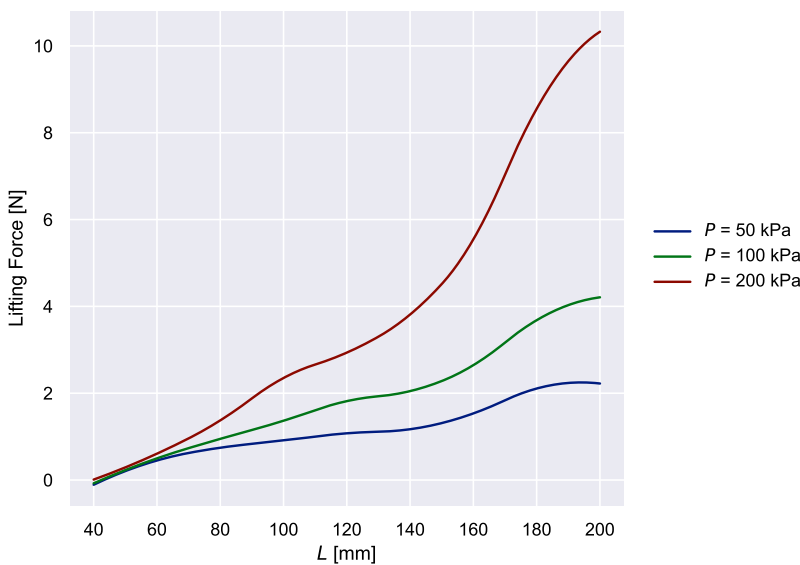

Figure 12. *Power characteristics of the developed model of the gripping device for flexible and porous objects at various parameters of inlet pressure.*

model (SI model) will utilize the following parameters: $H = 15$ mm, $D = 25$ mm, and $L = 40 - 200$ mm, to determine its characteristics (Fig. 12).

As shown in Fig. 12, the grasping force for flexible and porous objects remains linear throughout the entire range of channel length changes. This allows us to use the obtained modeling results (Fig. 12) for comparison with experimental data.

Using the experimental data obtained for materials Polyester 6, Flannel 3, and Linen 0 [52], the channel length of the model was determined, which correlates with the experimental materials (Table I). Based on the average value of the channel length determined for each material, approximate values were accepted: Polyester $6 - L = 100$ mm, Flannel $3 - L = 160$ mm, and Linen $0 - L = 140$ mm.

To analyze the reliability of the results obtained from the developed model compared to experimental data, graphical dependencies illustrating the influence of the grasping force on the inlet pressure are presented (Fig. 13).

Table I. *The ratio of the experimental to the channel length of the model.*

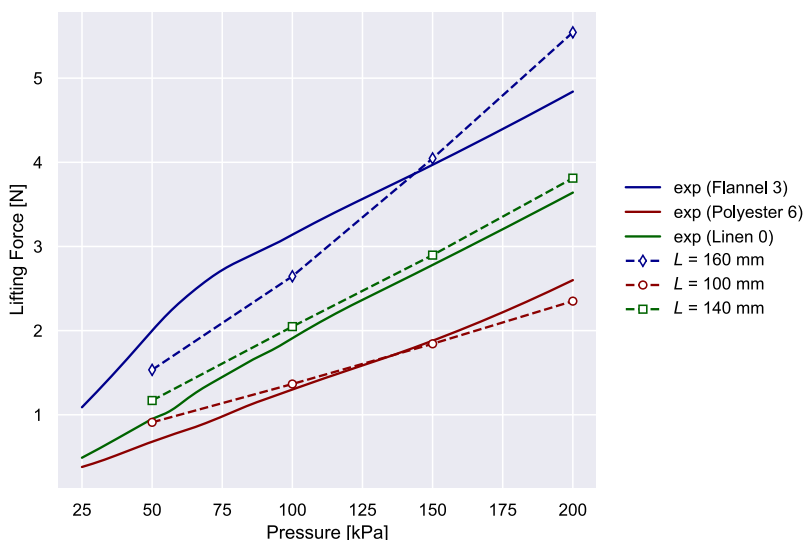|	Materials					
	Polyester 6		Flannel 3		Linen 0	
Pressure p_0 [kPa]	Exp. F [N]	Mod. L [mm]	Exp. F [N]	Mod. L [mm]	Exp. F [N]	Mod. L [mm]
50	0.68	75	2	170	1.15	130
100	1.3	95	3.14	170	1.91	130
200	2.6	110	4.84	155	3.64	140
Average value		94		165		133

Figure 13. *Influence of the inlet pressure of the gripping device on the lifting force for textile materials (experiment and modeling).*

The relative error between the simulation results and the experimental results was found to be 13%. It is acknowledged that in gas-dynamic modeling problems, an acceptable error can be up to 30%. Additionally, the flexibility and partial deformation of the textile material and insert during grasping and manipulation contribute to the increased error. Based on this, it can be concluded that the obtained modeling results are adequate, and the proposed model can be utilized for further research and optimization of grippers with similar designs.

The analysis of the obtained results of pressure and air velocity distribution is performed in a chamber that simulates a porous material (SI model, $H = 15$ mm, $D = 25$ mm, $L = 140$ mm, $p_0 = 100$ kPa) (Fig. 14(a)). The pressure in the chamber is observed along three lines: 1 – upper position, 2 – middle position, and 3 – lower position. The pressure distribution at different positions of the chamber in the model of the gripping device is examined (Fig. 14(b)).

As shown in Fig. 14(b), the pressure distribution along line 2 exhibits the same profile as along line 1. Pressure jumps in line 1 are formed due to the interaction of air flows through the holes of the anti-vibration insert, which is confirmed by the pressure distribution along line 1 in Fig. 15(a). However, the pressure distribution along line 2 is more stable, with no pressure jumps at the periphery. This is why, in the proposed methodology, the lifting force is determined based on the pressure distribution across the cross-section of the chamber's middle. Line 3 is not taken into account due to its lower vacuum caused
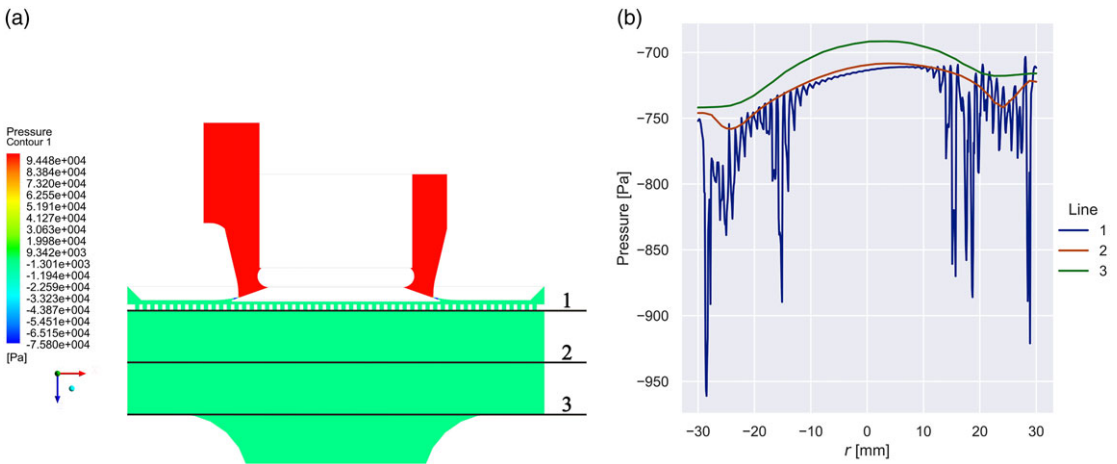
Figure 14. *Pressure distribution the cross-section of the model of the gripping device with marked position along the lines that pass.*
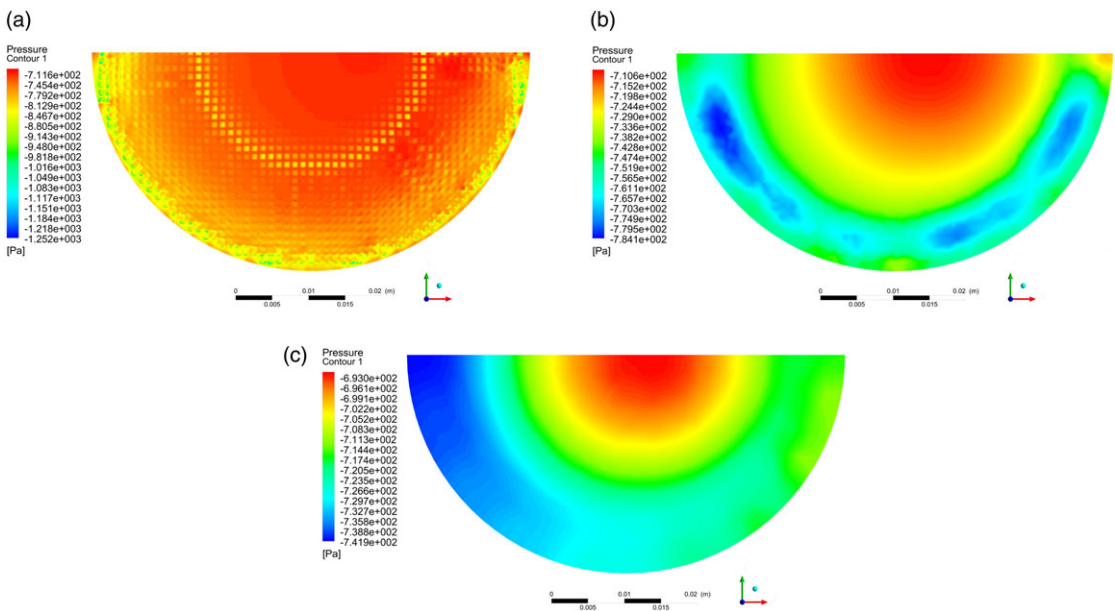

Figure 15. *Distribution of pressure on three sections of the chamber of the model of the gripping device: (a) 1 plane; (b) 2 planes; and (c) 3 planes.*

by its proximity to the channel. Furthermore, it can be observed that the pressure distribution is not symmetrical about the axis of the gripping device. This trend is consistent with other pressure parameters and changes in valve length. Therefore, the pressure distribution on the cross-sectional surfaces of the model gripping device's chamber is examined (Fig. 15).

From Fig. 15, it is evident that more vacuum is generated in the left part of the chamber. In particular, the experiment demonstrated that when manipulating the object, it tends to shift relative to the axis of the gripping device. The displacement occurs in the direction from which the air is supplied. The influence of the direction of the compressed air inlet is discussed in the paper [40]. For rigid objects, a slight increase in a vacuum on one side of the gripper has minimal impact on its grasping stability.
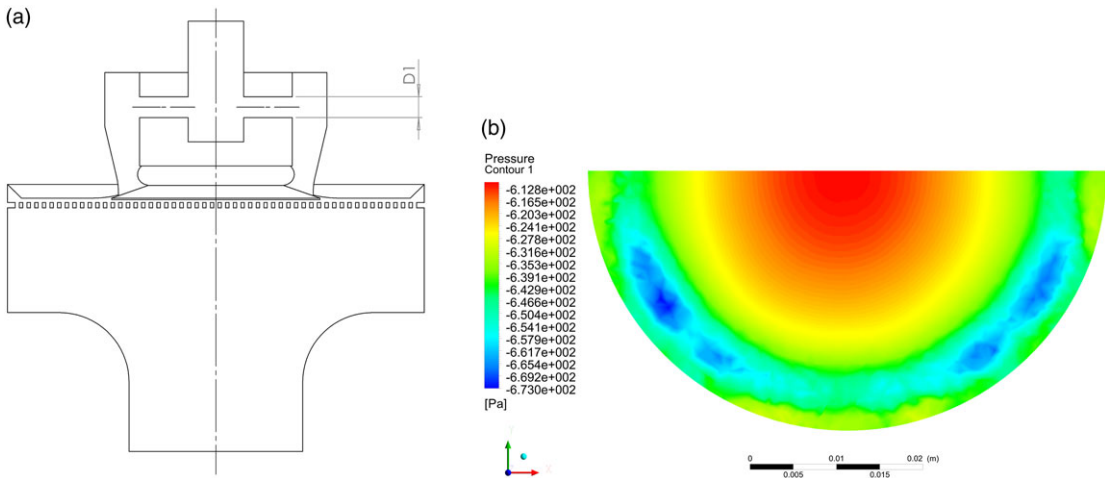
Figure 16. *modernized gripping device: (a) geometry and (b) pressure distribution in section 2 of the chamber.*

However, when handling light, flexible, and porous materials, this effect can cause significant displacement of the manipulated object relative to the grasping system. Therefore, this effect is undesirable for gripping devices designed for flexible and porous objects. To achieve an even distribution of airflow in the gripping device chamber, it is proposed to utilize a compressed air inlet through four radial holes with a diameter of $D1$ in the mounting of the conical insert (Fig. 16(a)).

Using the modernized model shown in Fig. 16(a) ($D1 = 3$ mm, SI model, $H = 15$ mm, $D = 25$ mm, $L = 140$ mm, $p_0 = 100$ kPa), the pressure distribution in the chamber (Plane 2) is determined, simulating the behavior of textile material (Fig. 16(b)).

The updated design of the gripper model is characterized by a uniform pressure distribution (Fig. 16(b)). However, the lifting force of the gripping device for this design will be lower than that of the previous design, as the pressure generated in the chamber is greater. Therefore, research was conducted to investigate the effect of the inlet pressure on the grasping force for different models (Fig. 17).

As can be seen from Fig. 17, the gripper for flexible and porous objects with pressure stabilization in the chamber has, on average, a 10% lower lifting force compared to the design with direct pressure supply to the chamber. This is because, when the supply pressure is applied through the fitting, compressed air does not directly enter the gripping chamber (Fig. 18).

Before the compressed air enters outlet chamber 13 of the gripping device, it passes through the small chamber 16 and the radial holes 17 in it, which reduces the energy of the airflow. However, despite the 10% reduction in the grasping force, the new design allows for increased gripping stability and minimizes object displacement during handling operations. It is still possible for the object of manipulation to experience displacement during the gripping process, as there are factors that affect this process regardless of the gripper's design. These factors include the positioning error of the gripping device relative to the horizontal plane, the displacement of the manipulation object's center of mass, the distance from which the gripper engages, the mechanical characteristics of the manipulation object, and the material from which it is made.

4. Conclusions

The article proposes a method for modeling gripping devices designed for flexible and porous objects using the FEM. The main parameters of the model that affect the lifting force and permeability of porous objects are identified. A special intermediately SST turbulence model is proposed to be used with a
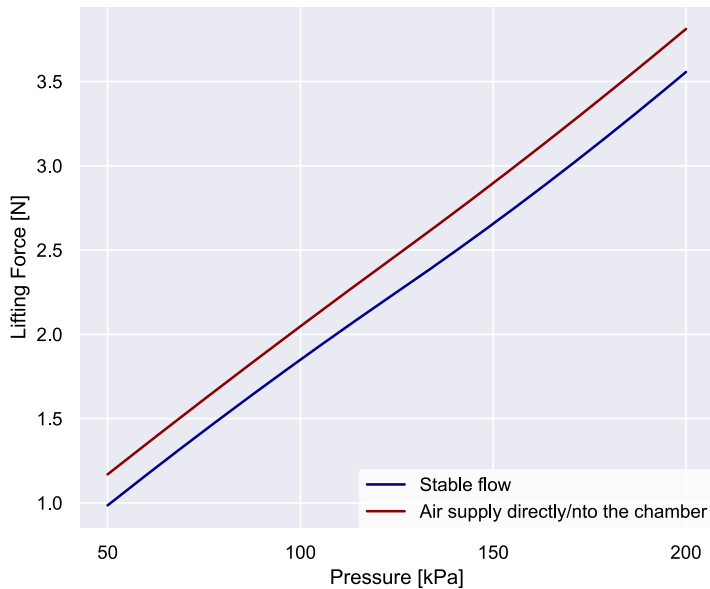
Figure 17. *Influence of inlet pressure on the lifting force of the gripper at various pressure supply designs.*
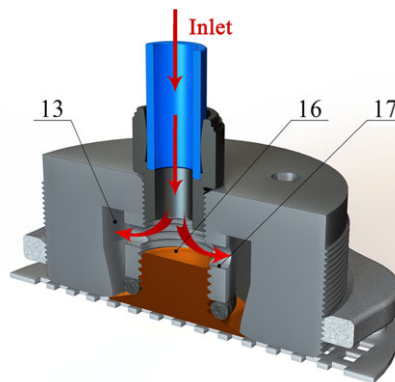

Figure 18. *Compressed air supply design with radial holes to stabilize the air pressure in the chamber of the gripping device for porous and flexible objects.*

minimum of 4 elements between adjacent planes of the model. Other model parameters for porous objects are determined by analyzing experimental simulation results: chamber height of 15 mm and channel diameter of 25 mm.

The power characteristics of the obtained model are determined for different supply pressures of the gripper while varying the length of the object channel. This allows for the simulation of compressed air flow changes through a porous object during manipulation. Using the obtained characteristics, the corresponding channel length is determined for three textile materials with different permeable properties. An experimental study is conducted, and the lifting force is compared with the obtained modeling data for three material samples. The relative error between the simulation results and the experimental results is found to be 13%. This error, considering the nature of gas-dynamic problems and flexible materials, indicates the adequacy of the results. One drawback of the proposed method is that when modifying

the parameters of the anti-vibration insert or the gap of the circular nozzle, it becomes necessary to reevaluate the appropriate parameters of the model for ensuring its adequacy.

Using the obtained modeling data, an analysis of the pressure distribution on the surface of the porous object during manipulation is performed. It is determined that the lifting force is unevenly distributed on the object's surface, leading to object displacement relative to the gripper's axis during gripping. This displacement is influenced by the parameters of compressed air entry into the gripper chamber. It is established that a system with radial holes for applying pressure to the gripper chamber should be used in the design of grippers for porous and flexible objects. This allows for the stabilization of pressure within the gripper chamber and achieves a symmetrical distribution of vacuum on the object's surface.

In the future, the proposed method will be used to investigate the influence of gripping device parameters on the vibration characteristics of manipulated objects and to optimize the active surface of the gripping device.

References

[1] V. E. Arriola-Rios, P. Guler, F. Ficuciello, D. Kragic, B. Siciliano and J. L. Wyatt, "Modeling of deformable objects for robotic manipulation: A tutorial and review," *Front. Robot. AI* **82**(7), 1–25 (2020). doi: 10.3389/frobt.2020.00082

[2] A. Bjornsson, M. Jonsson and K. Johansen, "Automated material handling in composite manufacturing using pick-and-place systems-a review," *Robot. Comput. Integr. Manuf.* **51**, 222–229 (2018).

[3] J. Sanchez, J.-A. Corrales, B.-C. Bouzgarrou and Y. Mezouar, "Robotic manipulation and sensing of deformable objects in domestic and industrial applications: A survey," *Int. J. Robot. Res.* **37**(7), 688–716 (2018).

[4] J. Borr'as, G. Aleny'a and C. Torras, "A grasping-centered analysis for cloth manipulation," *IEEE Trans. Robot.* **36**(3), 924–936 (2020).

[5] F. Nadon, A. J. Valencia and P. Payeur, "Multi-modal sensing and robotic manipulation of non-rigid objects: A survey," *Robotics* **7**(4), 74 (2018).

[6] M. Saadat and P. Nan, "Industrial applications of automatic manipulation of flexible materials," *Ind. Robot* **29**(5), 434–442 (2002).

[7] G. Seliger, F. Szimmat, J. Niemeier and J. Stephan, "Automated handling of non-rigid parts," *CIRP Ann.* **52**(1), 21–24 (2003).

[8] S. Donaire, J. Borras, G. Alenya and C. Torras, "A versatile gripper for cloth manipulation," *IEEE Robot. Autom. Lett.* **5**(4), 6520–6527 (2020).

[9] K. M. Digumarti, V. Cacucciolo and H. Shea, "Dexterous Textile Manipulation Using Electro-adhesive Fingers," **In:** *2021 IEEE/RSJ International Conference on Intelligent Robots and Systems (IROS)* (2021) pp. 6104–6109.

[10] E. W. Schaler, D. Ruffatto, P. Glick, V. White and A. Parness, "An Electrostatic Gripper for Flexible Objects," **In:** *2017 IEEE/RSJ International Conference on Intelligent Robots and Systems (IROS)* (2017) pp. 1172–1179.

[11] T. Yoneyama, T. Watanabe, H. Kagawa, J. Hamada, Y. Hayashi and M. Nakada, "Force Detecting Gripper and Flexible Micro Manipulator for Neurosurgery," **In:** *2011 Annual International Conference of the IEEE Engineering in Medicine and Biology Society* (2011) pp. 6695–6699.

[12] E. J. Park and J. K. Mills, "Dynamic Modeling of Flexible Payloads Grasped by Actuated Grippers Using Component Mode Synthesis," **In:** *Proceedings 2002 IEEE International Conference on Robotics and Automation* (2002) pp. 2443–2448.

[13] F. Osawa, H. Seki and Y. Kamiya, "Unfolding of massive laundry and classification types by dual manipulator," *J. Adv. Comput. Intel. Intel. Inf.* **11**(5), 457–463 (2007).

[14] Z. Hu, P. Sun and J. Pan, "Three-dimensional deformable object manipulation using fast online gaussian process regression," *IEEE Robot. Autom. Lett.* **3**(2), 979–986 (2018).

[15] A. Longhini, M. C. Welle, I. Mitsioni and D. Kragic, "Textile Taxonomy and Classification Using Pulling and Twisting," **In:** *2021 IEEE/RSJ International Conference on Intelligent Robots and Systems (IROS)* (2021) pp. 7564–7571.

[16] I. Garcia-Camacho, J. Borr'as, B. Calli, A. Norton and G. Aleny'a, "Household Cloth Object Set: Fostering Benchmarking in Deformable Object Manipulation," *IEEE Robot. Autom. Lett.* **7**(3), 5866–5873 (2022).

[17] S. Miller, J. Van Den Berg, M. Fritz, T. Darrell, K. Goldberg and P. Abbeel, "A Geometric Approach to Robotic Laundry Folding," *Int. J. Rob. Res.* **31**(2), 249–267 (2012).

[18] P. M. Taylor, "Presentation and gripping of flexible materials," *Assem. Autom.* **15**(3), 33–35 (1995).

[19] G. Fantoni, M. Santochi, G. Dini, K. Tracht, B. Scholz-Reiter, J. Fleischer, T. Kristoffer Lien, G. Seliger, G. Reinhart, J. Franke, H. Nørgaard Hansen and A. Verl, "Grasping devices and methods in automated production processes," *CIRP Ann.* **63**(2), 679–701 (2014).

[20] D. R. Kemp, P. M. Taylor and G. E. Taylor, "An Adaptive Sensory Gripper for Fabric Handling," **In:** *Proc. 4th IASTED Symp. on Robotics & Automation* (1984).

[21] F. Vercraene and P. Esquirol, "Analysis of a Ply Separation Gripper; Sensory Robotica for the Handling of Limb Materials," **In:** *NATO ASI Series F* (1990) pp. 127–136.

[22] G. J. Monkman, "Sensory integrated fabric ply separation," *Robotica* **14**(1), 114–125 (1996).

[23] K. Tai, A.-R. El-Sayed, M. Shahriari, M. Biglarbegian and S. Mahmud, "State of the art robotic grippers and applications," *Robotics* **5**(2), 11 (2016).

[24] R. Mykhailyshyn, V. Savkiv, P. Maruschak and J. Xiao, "A systematic review on pneumatic gripping devices for industrial robots," *Transport* **37**(3), 201–231 (2022).

[25] T. Lien, "Gripper Technologies for Food Industry Robots," **In:** *Robotics and Automation in the Food Industry* (2013) pp. 143–170.

[26] B. Willimon, I. Walker and S. Birchfield, "Classification of clothing using midlevel layers," *Int. Sch. Res. Not.* **2013**, 1–17 (2013).

[27] D. E. Canbay, P. Ferrentino, H. Liu, R. Moccia, S. Pirozzi, B. Siciliano and F. Ficuciello, "Calibration of Tactile/Force Sensors for Grasping with the Prisma Hand II," **In:** *2021 IEEE/ASME International Conference on Advanced Intelligent Mechatronics (AIM)* (2021) pp. 442–447.

[28] R. Mykhailyshyn, V. Savkiv, A. M. Fey and J. Xiao, "Gripping device for textile materials," *IEEE Trans. Autom. Sci. Eng.* (2022). doi: 10.1109/TASE.2022.3208796

[29] V. Savkiv, R. Mykhailyshyn, F. Duchon and O. Fendo, "Justification of design and parameters of bernoulli-vacuum gripping device," *Int. J. Adv. Robot. Syst.* **14**(6), 1729881417741740 (2017).

[30] V. Savkiv, R. Mykhailyshyn and F. Duchon, "Gasdynamic analysis of the bernoulli grippers interaction with the surface of flat objects with displacement of the center of mass," *Vacuum* **159**, 524–533 (2019).

[31] E. Toklu and F. Erzincanli, "Modeling of radial flow on a non-contact end effector for robotic handling of non-rigid material," *J. Appl. Res. Technol.* **10**(4), 590–596 (2012).

[32] S. Davis, J. Gray and D. G. Caldwell, "An end effector based on the bernoulli principle for handling sliced fruit and vegetables," *Robot. Comput. Integr. Manuf.* **24**(2), 249–257 (2008).

[33] A. Petterson, T. Ohlsson, D. G. Caldwell, S. Davis, J. O. Gray and T. J. Dodd, "A Bernoulli principle gripper for handling of planar and 3D (food) products," *Ind. Robot.* **37**(6), 518–526 (2010).

[34] R. Sam and N. Buniyamin, "A Bernoulli Principle Based Flexible Handling Device for Automation of Food Manufacturing Processes," **In:** *2012 International Conference on Control, Automation and Information Sciences (ICCAIS)* (2012) pp. 214–219.

[35] X. F. Brun and S. N. Melkote, "Evaluation of Handling Stresses Applied to EFG Silicon Wafer using a Bernoulli Gripper," **In:** *IEEE 4th World Conference on Photovoltaic Energy Conference* (2006) pp. 1346–1349.

[36] X. Brun and S. Melkote, "Effect of substrate flexibility on the pressure distribution and lifting force generated by a bernoulli gripper," *J. Manuf. Sci. Eng.* **134**(5), 051010 (2012).

[37] D. Liu, C. S. Teo, W. Liang and K. K. Tan, "Soft-acting, noncontact gripping method for ultrathin wafers using distributed bernoulli principle," *IEEE Trans. Autom. Sci. Eng.* **16**(2), 668–677 (2018).

[38] G. Dini, G. Fantoni and F. Failli, "Grasping leather plies by bernoulli grippers," *CIRP Ann.* **58**(1), 21–24 (2009).

[39] S. Erturk and G. Samtas, "Design of grippers for laparoscopic surgery and optimization of experimental parameters for maximum tissue weight holding capacity," *Bull. Polish Acad. Sci. Tech. Sci.* **67**(6), 1125–1132 (2019).

[40] R. Mykhailyshyn and J. Xiao, "Influence of inlet parameters on power characteristics of bernoulli gripping devices for industrial robots," *Appl. Sci.* **12**(14), 7074 (2022).

[41] V. Savkiv, R. Mykhailyshyn, P. Maruschak, V. Kyrylovych, F. Duchon and L. Chovanec, "Gripping devices of industrial robots for manipulating offset dish antenna billets and controlling their shape," *Transport* **36**(1), 63–74 (2021).

[42] V. Savkiv, R. Mykhailyshyn, F. Duchon, P. Maruschak and O. Prentkovskis, "Substantiation of Bernoulli Grippers Parameters at Non-Contact Transportation of Objects with a Displaced Center of Mass," **In:** *Transport Means 2018: Proceedings of the 22nd International Scientific Conference* (2018) pp. 3–5.

[43] R. Mykhailyshyn, V. Savkiv, I. Boyko, E. Prada and I. Virgala, "Substantiation of parameters of friction elements of bernoulli grippers with a cylindrical nozzle," *Int. J. Manuf. Mater. Mech. Eng.* **11**(2), 17–39 (2021).

[44] V. Savkiv, R. Mykhailyshyn, F. Duchon, V. Piscio, V. Medvid and I. M. Diahovchenko, "Investigation of the Accuracy of the Base of the Object of Manipulation of Bernoulli Gripping Devices," **In:** *2021 IEEE 3rd Ukraine Conference on Electrical and Computer Engineering (UKRCON)* (2021) pp. 421–425.

[45] K. Shi and X. Li, "Experimental and theoretical study of dynamic characteristics of bernoulli gripper," *Prec. Eng.* **52**, 323–331 (2018).

[46] R. Mykhailyshyn, V. Savkiv, F. Duchon and L. Chovanec, "Experimental Investigations of the Dynamics of Contactless Transportation by Bernoulli Grippers," **In:** *2020 IEEE 6th International Conference on Methods and Systems of Navigation and Motion Control (MSNMC)* (2020) pp. 97–100.

[47] K. Shi and X. Li, "Optimization of outer diameter of bernoulli gripper," *Exp. Therm. Fluid. Sci.* **77**, 284–294 (2016).

[48] T. Giesen, E. Burk, C. Fischmann, W. Gauchel, M. Zindl and A. Verl, "Advanced gripper development and tests for automated photovoltaic wafer handling," *Assem. Autom.* **33**(4), 334–344 (2013).

[49] X. Yu and X. Li, "Inertia-enhancement effect of divergent flow on the force characteristics of a bernoulli gripper," *Phys. Fluids* **33**(5), 057108 (2021).

[50] R. Mykhailyshyn, F. Duchoň, I. Virgala, P. J. Sinčák and A. M. Fey, "Optimization of outer diameter bernoulli gripper with cylindrical nozzle," *Machines* **11**(6), 667 (2023).

[51] R. Mykhailyshyn, F. Duchoň, M. Mykhailyshyn and A. M. Fey, "Three-dimensional printing of cylindrical nozzle elements of bernoulli gripping devices for industrial robots," *Robotics* **11**(6), 140 (2022).

[52] R. Mykhailyshyn, Substantiation Parameters of Gripping Devices of Industrial Robots and Methods of Manipulation of Flexible Objects. https://romanmykhailyshyn.github.io/portfolio/portfolio-1/ (Accessed: 18 May 2023).

[53] S. Cant, "High-performance computing in computational fluid dynamics: Progress and challenges," *Philos. Trans. A Math. Phys. Eng. Sci.* **360**(1795), 1211–1225 (2002).

[54] J. Aubin, D. F. Fletcher and C. Xuereb, "Modeling turbulent flow in stirred tanks with CFD: The influence of the modeling approach, turbulence model and numerical scheme," *Exp. Therm. Fluid. Sci.* **28**(5), 431–445 (2004).

[55] F. R. Menter, "Two-equation eddy-viscosity turbulence models for engineering applications," *AIAA J.* **32**(8), 1598–1605 (1994).

[56] F. Menter, T. Esch and S. Kubacki, "Transition modelling based on local variables," *Eng. Turbul. Model. Exp.* **5**, 555–564 (2002).

[57] F. R. Menter, R. Langtry and S. Volker, "Transition modelling for general purpose CFD codes," *Flow Turbul. Combust.* **77**(1), 277–303 (2006).